Optics & Laser Technology 184 (2025) 112528

Contents lists available at ScienceDirect

Optics and Laser Technology

journal homepage: www.elsevier.com/locate/optlastec

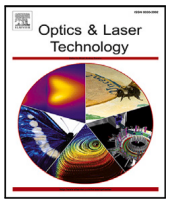

Full length article

Comprehensive intensity and phase noise analysis of a femtosecond Cr:ZnSe Kerr-lens mode-locked laser

Dario Giannotti [a,*], Antonio Caruso [a,b], Fedele Pisani [a,b], Francesco Canella [b], Niccolò S. Barberio [a], Alessio Gambetta [a,b], Nicola Coluccelli [a,b], Yuchen Wang [c], Paolo Laporta [a,b], Gianluca Galzerano [b]

[a] Dipartimento di Fisica, Politecnico di Milano - Piazza Leonardo da Vinci, 32, 20133 Milano, Italy
[b] Istituto di Fotonica e Nanotecnologie, CNR - Piazza Leonardo da Vinci, 32, 20133 Milano, Italy
[c] Shanghai Institute of Optics and Fine Mechanics, Chinese Academy of Sciences - Shanghai 201800, China

ARTICLE INFO

Keywords:
Ultrafast mid-infrared laser
Kerr-lens mode-locked laser
Laser intensity noise measurements
Low time jitter mode-locked lasers

ABSTRACT

We present a comprehensive characterization of a Kerr-lens mode-locked ultrafast Cr:ZnSe laser that generates nearly transform-limited pulse trains with a duration of 42 fs and an optical bandwidth of 8.2 THz, at an emission wavelength of 2.4 μm and 213 MHz repetition frequency. Our detailed investigation of intensity noise and pulse repetition-rate phase noise underscores the exceptional spectral purity of the Cr:ZnSe laser, even when pumped by a multi-longitudinal mode Er-fiber laser. This remarkable performance is attributed to the efficient random second harmonic generation mechanism within the ZnSe polycrystal, which significantly mitigates the transfer of pump laser intensity noise to the Cr:ZnSe laser, achieving in the mode-locking regime more than 13 dB pump noise attenuation in the Fourier bandwidth from 10 Hz to 10 MHz, also resulting in the complete suppression of the Cr:ZnSe resonance relaxation oscillations. Additionally, we report on the frequency stabilization of the pulse repetition frequency against an RF rubidium clock, down to a fractional frequency stability of 2×10^{-11} for an integration time of 10 s, demonstrating a pulse jitter of less than 1.6 ps over an integration bandwidth from 100 Hz to 100 MHz.

1. Introduction

High-spectral purity ultrafast laser systems operating in the mid-infrared (MIR) spectral region (2-20 μm) find a variety of applications in high-precision and broad optical bandwidth sensing and spectroscopy [1–3]. In this framework, the reduction of intensity and phase noises plays a primary role in enhancing performance. In the 2-3 μm strategic wavelength range, where the main transitions of the fundamental vibrational modes of C-H bonds fall, the Cr^{2+}-doped ZnS/ZnSe lasers exhibit broad emission bandwidths able to sustain the generation of few optical cycle pulses [4,5]. Following the first demonstration of femtosecond Cr:ZnSe lasers [6], this polycrystal has aroused interest in the community. This is partly due to its efficient random quasi-phase matching second harmonic generation (SHG) and other three-wave mixing processes, such as third and fourth harmonic conversions as well as parametric sum and difference frequency process [7,8] that allows the production of broadband light in a multi-wavelength spectral region. In addition, the efficient intracavity random quasi-phase matching SHG process, an instantaneous nonlinear loss mechanism, is beneficial in strongly suppressing both pump laser noise and laser relaxation oscillations [9,10]. While Kerr-lens mode-locked Cr:ZnSe lasers have demonstrated remarkable performance in terms of pulse duration and output power [11–15], investigating their noise characteristics, especially intensity and phase noise, is equally crucial. Understanding the noise performance of this kind of lasers is essential for ensuring their reliability in high-sensitivity applications such as broadband spectroscopy or imaging for high-precision chemical species identification and detection. Indeed, although other KLM-mode-locked laser systems, such as Ti:sapphire, Yb-, and Ho-doped crystals [16–18], have demonstrated excellent performance in terms of low-intensity noise and pulse jitter (for example the KLM Ho-doped laser demonstrated integrated relative intensity noise of 0.02% and a RMS phase noise 0.543 mrad in the bandwidth from 10 Hz to 10 MHz [18]), the presence of the random second harmonic effect in Cr:ZnSe (and also Cr:ZnS) lasers enables the complete suppression of relaxation oscillations [10]. These oscillations, on the other hand, are present in the aforementioned systems and limit their ultimate performance as predicted by Ref. [19].

* Corresponding author.
E-mail address: dario.giannotti@polimi.it (D. Giannotti).

https://doi.org/10.1016/j.optlastec.2025.112528
Received 7 November 2024; Received in revised form 8 January 2025; Accepted 21 January 2025
Available online 1 February 2025

Here we report on a detailed experimental investigation of the intensity and phase noise in a Kerr-lens mode-locked (KLM) Cr:ZnSe laser source at 2.4 μm wavelength, generating pulse trains at 213 MHz repetition frequency with a duration of 42 fs and an optical bandwidth of 8.2 THz. In the KLM regime, the Cr:ZnSe laser strongly suppresses the intensity noise originating from the multi-longitudinal mode Er-fiber laser pump. The reduction of the intensity noise of the Er pump laser has been described in the Fourier frequency range from 10 Hz to 10 MHz showing an average value higher than 13 dB. For Fourier frequencies at around 1 kHz and larger than 1 MHz, the mode-locked Cr:ZnSe laser is characterized by relative intensity noise (RIN) levels of −135 dB/Hz and −145 dB/Hz, respectively. A comparison between the RIN of the Cr:ZnSe laser in mode-locked and CW regimes is also performed confirming that the noise suppression of the random SHG process is even more efficient with respect to the peak of the relaxation oscillations. In this case, suppression of 27 dB is measured at around 1 MHz, coinciding with the CW relaxation oscillation peak. Finally, frequency stabilization of the pulse repetition frequency against an RF rubidium clock is also performed demonstrating a pulse jitter lower than 1.6 ps in the integration bandwidth from 100 Hz to 100 MHz.

2. Experimental setup

Fig. 1 shows the experimental setup of the KLM Cr:ZnSe laser. The 5-mirror linear cavity resonator lies in an airtight chamber, allowing a nitrogen atmosphere. It consists of two plane high-reflectivity chirped mirrors (PM), two plano-concave chirped mirrors with a radius of curvature of 50 mm (CM), and a plane 3% output coupler (OC). The chirped mirrors have a specifically designed group-delay dispersion (GDD) of -240±20 fs^2 to control the overall intracavity dispersion, essential for the soliton-like pulse formation. The pump radiation is a multi-mode Er-fiber laser (ELM-20-LP IPG Photonics) centered at 1.57 μm wavelength, with a maximum output power of 20 W. The pump laser reaches the laser resonator through a broadband CaF_2 window (transmission > 95% at the pump wavelength) and is focused on the Cr:ZnSe crystal through the 50-mm curved mirror (transmittance of 70% at 1.57 μm) by an AR-coated (1.05-1.7 μm) 40-mm plano-convex lens (L). The active medium (dimensions $2.8 \times 4.9 \times 5.0$ mm, doping $N_{Cr} = 9.2 \times 10^{18}$ cm^{-3}) is inserted at the Brewster angle (67.7° at 2.4 μm) between the two curved mirrors. The crystal is mounted on a Peltier-cooled copper holder maintained at a constant temperature of 20°C. The resonator is in an asymmetric X-configuration with arm lengths of 40.4 cm and 15.8 cm, respectively. The folding angles of the curved mirrors are 14° and 16° to compensate for the astigmatism introduced by the incidence at the Brewster angle on the active crystal. Soft-aperturing KLM is obtained by operating the laser resonator with a distance between the curved mirrors within a range of 54.5 mm to 56.1 mm, corresponding to the second stability region of the cavity. The propagation length through the Cr:ZnSe is 3.19 mm, resulting in a GDD of 1260 fs^2 per round trip along the optical path. Considering the chirped mirrors' dispersion, the total calculated net GDD of the resonator is about −260 fs^2, allowing for a solitonic mode-locking regime.

First, we characterized the Cr:ZnSe laser setup operating in continuous wave (CW), moving the cavity at the center of the second stability zone and aligning the optical elements to maximize the transmitted fluorescence (broad-spectrum emission from 2.0 μm to 2.4 μm). Then, we increased the distance between the curved mirrors to bring the cavity to the edge of the second stability zone, where the geometric dimensions of the beam allow a soft-aperture KLM. The "self-starting" mode-locking (ML) is achieved by perturbing the ending mirror of the long arm of the resonator, mounted on a translation stage. By slightly shifting the position of the Cr:ZnSe polycrystal along the resonator propagation axis, the KLM regime is optimized to maximize the pulse spectrum and reduce the relative intensity noise, striking a balance between the additional gain due to the Kerr lens and the increase in nonlinear losses due to random phase-matched SHG in the Cr:ZnSe polycrystal. A fast photodetector and an InGaAs spectrometer (NIRquest) were placed after the OC to confirm the transition to the ML regime. During this process, the photodetector revealed a pulse train in the time domain with a repetition frequency of 213 MHz, while the spectrometer monitored the broadening of the Cr laser in the spectral domain. The ML regime starts at an incident pump power threshold of 2.5 W. The maximum average output power in a single-pulse soliton regime was 190 mW with an incident pump power of 2.7 W, corresponding to a laser slope efficiency of 11%. We observed a multi-pulse regime at higher incident pump power levels. Fig. 2 reports the spectrum of the KLM Cr:ZnSe laser at the average output power of 190 mW as recorded by a Fourier Transform Infrared (FTIR) spectrometer (JASCO FT/IR 6800) with a resolution of 1 cm^{-1} (30 GHz) in a frequency span from 85 to 300 THz (corresponding to a wavelength range from 1 to 3.5 μm). Fig. 2 shows both the main peak at the fundamental wavelength of 2410 nm and its second harmonic, with FWHMs of 180 nm (9.3 THz) and 67 nm (13.8 THz), respectively. At 190 mW average output power, the SHG beam at the laser output has an average power of 8.5 mW, corresponding to a single-pass intracavity SHG power of 59.3 mW (as calculated using the measured OC transmission and chirped mirror reflectivity, 53% and 27%, respectively, at 1.2 μm). It is worth noting that the Cr:ZnSe laser is characterized by an extremely wide optical emission bandwidth covering the range from 2.0 to 3.2 μm (more than 60 THz) at −35 dB. Besides the random quasi-phase-matched SHG signal, the nonlinearity of the Cr:ZnSe polycrystal is also evident by the sidebands around the residual pump signal, at ±12 THz due to the cross-phase modulation between the CW pump laser and the intracavity ultrashort Cr:ZnSe laser [20]. In the frequency region between 109 THz and 120 THz, we observed several absorption lines, which are attributed to intracavity water vapor.

Fig. 3(a) presents a detailed view of the spectrum at the fundamental wavelength acquired with the cavity resonator closed in the airtight chamber and maintained in a nitrogen atmosphere with continuous flow. The nitrogen atmosphere allows a strong reduction of the water vapor absorption, leading to a high-purity spectral profile. The ML pulse spectrum is shifted around 123.9 THz (2419 nm wavelength), with a spectral bandwidth of 8.2 THz (158 nm). In the same operating conditions, Fig. 3(b) shows the interferometric autocorrelation trace (blue line) and the envelop fitting profile (orange line) of the KLM Cr:ZnSe laser. Assuming a $sech^2$ pulse shape, the envelope FWHM of 60 fs matches a pulse duration of 42 fs (time constant $t_p = 24$ fs), equivalent to approximately five optical cycles at the peak wavelength of 2.4 μm. The relative time-bandwidth product is 0.340, close to the 0.315 value of the Fourier limit of the $sech^2$ pulse, indicating a small residual chirp in the KLM Cr:ZnSe pulses. The latter was estimated using the modified-spectrum auto interferometric correlation method (MOSAIC) [21] introducing the chirp parameter β, defined by the phase acquired due to the frequency chirp $\phi_{chirp} = \beta(t^2/t_p^2)$. In brief, the MOSAIC technique improves the measurability of the chirp from interferometric autocorrelation traces by first Fourier transforming the interferogram, then filtering out the fundamental frequency component of the autocorrelation trace, and finally by antitransforming the residual DC and second harmonic components. The resulting filtered interferogram easily converges as a function of the chirp parameter β, estimated below 0.2 rad.

3. Relative intensity noise measurement

The measurement of the power spectral density of the relative intensity noise (RIN) of the KLM Cr:ZnSe is performed using an extended InGaAs photodetector with a bandwidth of 25 MHz (PDA10D2 Thorlabs) and an electronic spectrum analyzer (ESA, Agilent E4445A). Fig. 4(a) shows the RIN power spectral densities in the Fourier frequency range from 10 Hz to 10 MHz of the Er-fiber pump (red line) and the Cr:ZnSe laser in CW (blue line) and KLM (green line) regimes,

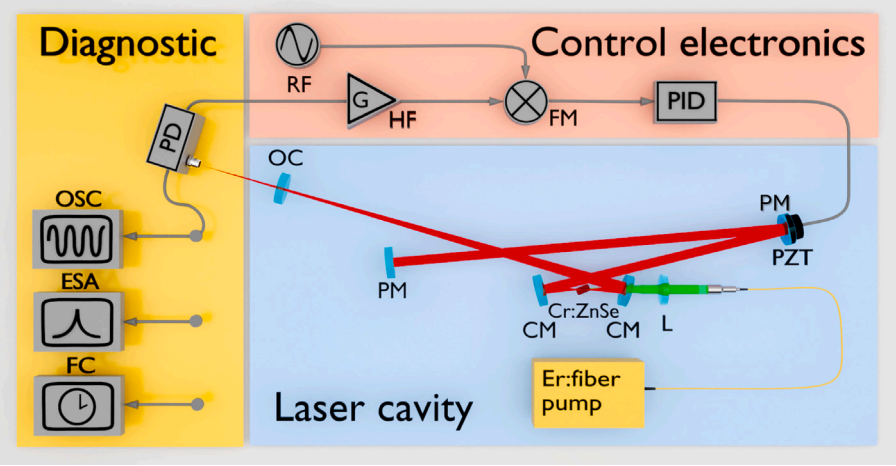

Fig. 1. Experimental setup of the KLM Cr:ZnSe laser. PD, photodiode. OSC, oscilloscope. ESA, electronic spectrum analyzer. FC, frequency counter. RF, radio frequency generator. HF, high-frequency amplifier. FM, frequency mixer. PID, proportional–integral–derivative controller. OC, output coupler. PM, plane mirror. CM, curved mirror. PZT, piezoelectric transducer. L, pump lens.

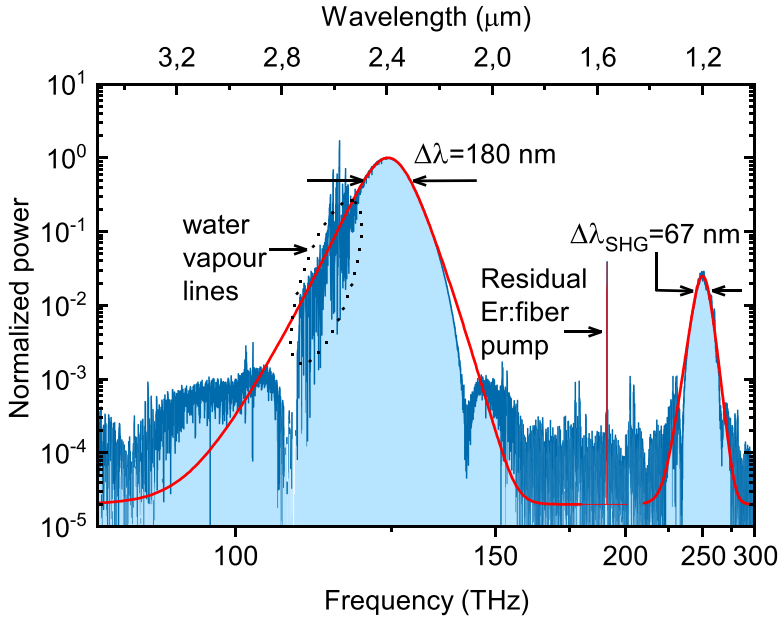

Fig. 2. Output spectrum of the KLM Cr:ZnSe laser, in ambient atmospheric conditions, recorded with a FTIR spectrometer at a resolution of 1 cm^{-1} and averaged over five samples. The noticeable intensity modulation in the frequency region from 109 to 120 THz is due to intracavity water absorption lines. The red lines are the intensity fits of the acquired data, considering hyperbolic secant profiles of the fundamental and SHG pulses.

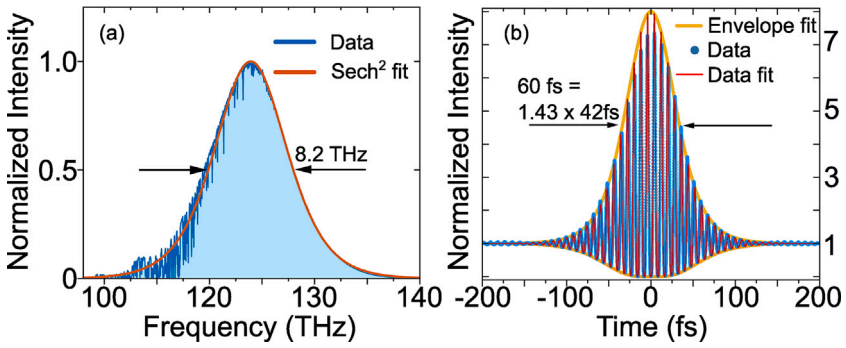

Fig. 3. Pulses characterization in nitrogen purged atmosphere: (a) spectral profile of the KLM Cr:ZnSe laser and (b) interferometric two-photon autocorrelation. The red curves are the intensity fits of the acquired data (blue lines), considering a secant hyperbolic profile of the pulse.

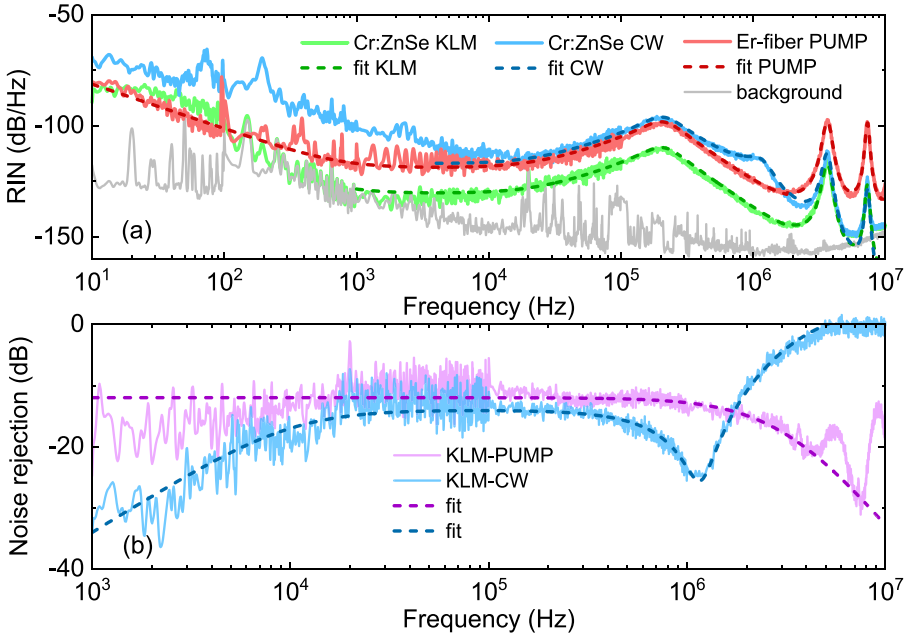

Fig. 4. RIN characterization: (a) RIN power spectral densities from 10 Hz to 10 MHz acquired for the pump laser (red) and the Cr:ZnSe laser both in CW (light blue) and KLM (green) regime. The gray line is the reference background. (b) Calculated noise rejection transfers from pump laser and CW regime to KLM. The fits (dashed line) agree with the theoretical curves computed using equation 2 of Ref. [10].

together with the measurement background noise floor (photodetector dark current noise). The spectral profile of the RIN of the pump Er-fiber laser presents a $1/f^2$ trend for frequencies lower than 1 kHz, a broad resonance peak of −99 dB/Hz at 203 kHz (corresponding to the resonant relaxation oscillations, RROs), and two pronounced peaks in the high-frequency limit, at 3.5 MHz (−98 dB/Hz) and 7 MHz (−99 dB/Hz), respectively (due to the mode-beating of the multi-longitudinal mode laser regime). The noise of the Er-doped fiber laser mainly consists of the vacuum noise resulting from the output coupling, the dipole fluctuation noise, the pump source intensity noise, and the spontaneous emission from the excited state level to the ground level. Indeed, we were able to fit with excellent accuracy the measured Er-fiber RIN power spectral density with the intensity noise transfer function reported in Ref. [22], as shown Fig. 4(a) (fit Er-laser curve). Specifically, the Er-fiber RRO peak is characterized by a pair of complex conjugate poles, with an oscillation frequency of 210 kHz and a damping ratio of 0.33, and from a zero at the frequency of 22.3 kHz. In contrast, the two mode-beating peaks are described by a Lorentzian function.

Fig. 4(a) shows the RIN of the Cr:ZnSe laser both in the KLM and CW regimes. Concerning the CW regime, obtained with the same cavity configuration as for the KLM action, the RIN is higher than that of the Er-fiber pump for Fourier frequencies lower than 10 kHz, due to the high sensitivity to acoustic and vibrational noise of the laser resonator operating close to the edge of the second stability zone, which corresponds also to a lower gain in the Cr:ZnSe crystal and higher intracavity diffraction losses respect to the KLM regime. At higher frequencies, the RIN is dominated by the Er fiber RRO pump noise, while the two pump-beating peaks are attenuated by 14 dB and 25 dB, respectively. In addition, a new peak at −114 dB/Hz appears at approximately 1.18 MHz, corresponding to the RRO peak of the Cr:ZnSe laser (a pair of complex conjugate poles, with an oscillation frequency of 1.18 MHz and a damping value of 0.21). When the Cr:ZnSe laser switches from the CW to the KLM regime a remarkable noise reduction is observed across the full Fourier frequency range, due to the combination of different mechanisms such as Kerr-lens induced increase of the optical gain and reduction of resonator diffraction losses, non-linear losses mainly due to SHG and eventually THG. In particular, the RIN power spectral density in KLM is reduced compared to the Er fiber pump noise by more than 10 dB, reaching a noise rejection value larger than 20 dB for frequencies higher than 3 MHz. Furthermore, in the KLM regime, the RRO of the Cr:ZnSe laser system is clamped by 25 dB mainly ascribed to the efficient random SHG mechanism within the ZnSe polycrystal (the measured SHG efficiency is 1.9%, nearly two times higher than the efficiency reported in Ref. [10], which used a 5-mm thick Cr:ZnS polycrystal). To better highlight the transfer noise function between the Er-fiber pump and the Cr:ZnSe laser system, Fig. 4(b) shows the measured intensity noise rejection between the KLM Cr:ZnSe laser with respect to the Er-fiber pump laser and the CW Cr:ZnSe laser (computed as the difference between the related RIN power spectral densities), along with the theoretical curves that best fit the experimental data. The figure reports the data starting from a Fourier frequency of 1 kHz because the RIN spectrum of the KLM Cr:ZnSe is limited by the background dark current noise of the InGaAs photodetector. The curves demonstrate pump noise rejection of −13 dB over a spectrum from 1 kHz up to 1 MHz, which increases further for higher frequencies due to the low-pass filtering of the Cr:ZnSe system. From the comparison between the KLM and CW regimes of the Cr:ZnSe laser, it is worth noting that the combination of Kerr-lens effect (optical gain increases and reduction of the intracavity losses) together with the random SHG process in the Cr:ZnSe laser, which introduces an instantaneous nonlinear loss perturbing the dynamic observed in CW, strongly suppresses the RRO of the Cr:ZnSe, following the recent results reported in [10]. It is important to highlight that, although the SHG process is instantaneous, i.e., broadband, the effect of pump noise reduction is instead modulated by the spectral response of the Cr:ZnSe laser system, as reported in [10]. The experimental data shown in Fig. 4(b) (light blue curve) agree well with the theory reported in [10], showing a reduction in noise suppression for Fourier frequencies higher than 4 MHz. Finally, the integrated relative intensity noise of the measured KLM RIN spectrum, numerically calculated, is below 0.16% in the bandwidth from 10 Hz to 10 MHz, which is nearly ten times lower than the 1.2% value for the Er fiber pump laser. This low-intensity noise value of the KLM Cr:ZnSe laser is still mainly due to the multimode beating and RRO noise originating from the pump laser, which accounts for a residual contribution of 0.1%.

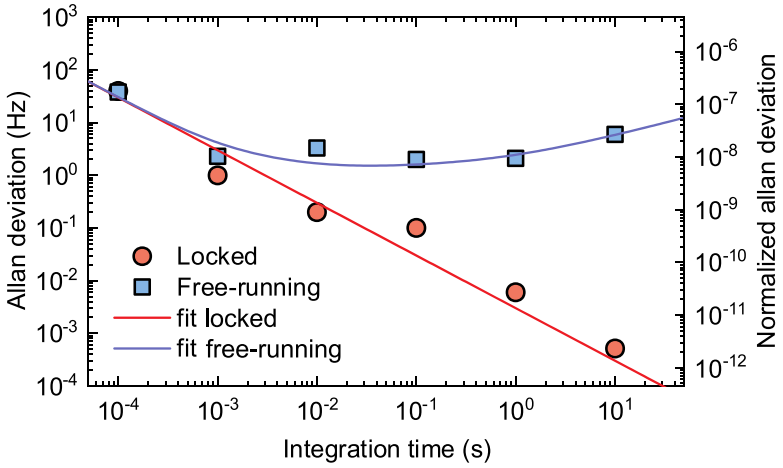

Fig. 5. Allan variance of the pulse repetition frequency in free-running and in locked conditions, respectively. Continuous lines represent the best curve fittings: $\sigma(\tau)_{\Delta\nu} = (5\times10^{-6}\tau^{-1} + 2 + 3\tau)^{1/2}$ and $\sigma(\tau)_{\Delta\nu} = 3\times10^{-3}\tau^{-1}$ in free-running and locked conditions, respectively.

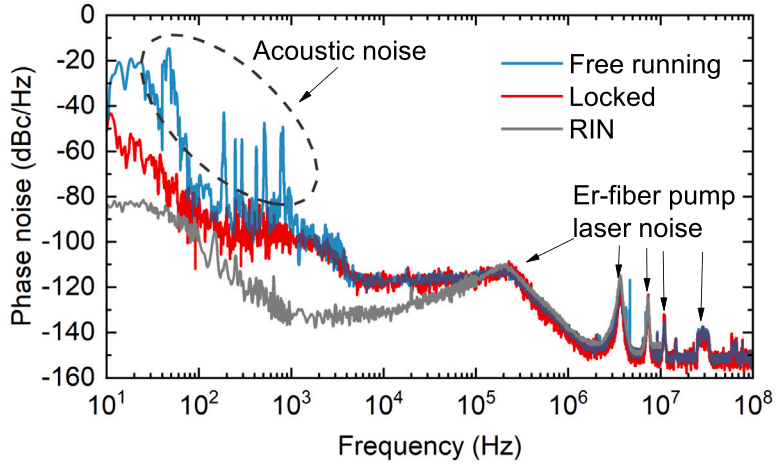

Fig. 6. Power spectral density of the phase noise of the pulse repetition frequency. The blue and red lines refer to the unlocked and locked conditions, respectively, whereas the gray curve represents the RIN spectrum.

4. Repetition frequency stabilization and phase noise measurement

Following the scheme reported in Fig. 1, the repetition frequency of the KLM Cr:ZnSe laser can be actively stabilized against an RF synthesizer. More in detail, the ultrafast pulse train is detected using a 1-GHz bandwidth extended InGaAs photodiode whose output signal is sent to a mixer (Mini-Circuits ZAD-1+) and compared to a reference RF synthesizer (Rohde & Schwarz SMT 06). The mixer output signal is sent through a low-pass 1-MHz bandwidth filter to a proportional-integrative-derivative servo that controls a piezo-electric high-voltage amplifier acting on a laser cavity mirror. To characterize the stability of the pulse repetition frequency and its phase noise power spectral density, the photodiode output is also sent to an electronic frequency counter and an electrical spectrum analyzer equipped with the phase noise measurement capability (Agilent 53230A).

Fig. 5 shows the Allan deviation, $\sigma(\tau)_{\Delta\nu}$ in Hz unit, of the pulse repetition frequency as a function of the integration time τ, as computed by the electronic frequency counter. In free-running conditions (blue squares), the Allan deviation ranges from 40 to 2 Hz in the explored integration time from 0.1 ms to 10 s. The data can be well interpolated by the following polynomial equation: $\sigma(\tau)_{\Delta\nu} = (h_0\tau^{-1} + h_{-1} + h_{-2}\tau)^{1/2}$, where $h_0 = 5\times10^{-6}$ Hz, $h_{-1} = 2$ Hz^2, and $h_{-2} = 3$ Hz^3 are the polynomial coefficient of the white, flicker, and random walk frequency noise contributions [23]. When the frequency stabilization loop is activated, the Allan deviation drops and it is characterized by a trend $\sigma(\tau)_{\Delta\nu} = H/\tau$, where $H = 3\times10^{-3}$, due to a white phase noise contribution [23] reaching a stability level of 0.5 mHz (2×10^{-11} in fractional terms) at 10 s integration time. We achieve a more comprehensive characterization of the short-term stability of the pulse repetition frequency by conducting a frequency domain measurement. Fig. 6 reports the power spectral densities of the phase noise associated with the pulse repetition frequency in free-running and locked conditions, as measured by the electrical spectrum analyzer (L-script power spectral density) in the frequency range from 10 Hz to 100 MHz. For comparison, Fig. 6 also presents the RIN power spectral density, indicating that for Fourier frequency higher than 100 kHz the measurement is limited by the laser RIN. In both the free-running and locked conditions the phase noise power spectral density is white in the range from 10 to 100 kHz at a level of −117 dBc/Hz. In the free-running case, the phase noise increases with a power law f^{-2} for frequencies lower than 10 kHz. Down to 100 Hz, additional contributions appear due to acoustic noise acting on the Cr:ZnSe resonator. Acoustic noise is, in contrast, strongly suppressed when the repetition frequency is stabilized against the RF

synthesizer up to a control loop bandwidth of ~1 kHz. From the power spectral densities of the phase noise of the repetition frequency, root-mean-square (RMS) phase noise of 0.7 rad and 15 mrad are computed in the integration bandwidth from 10 Hz to 100 MHz for the free-running and locked conditions respectively. In both cases, more than 95% integrated phase noise originates from the contribution within the bandwidth of 10 Hz and 100 Hz, thus the 1-kHz control loop adopted is well suited to reject this major low-frequency noise contribution by a factor of 50. In particular, the integrated phase noise in the bandwidth from 100 Hz to 100 MHz is 2.17 mrad in locked conditions, corresponding to a timing jitter of the repetition frequency of less than 1.6 ps.

5. Conclusion

In conclusion, we report on a detailed characterization of the intensity and phase noise properties of a Kerr-lens mode-locked Cr:ZnSe laser generating a pulse train at 2.4 μm wavelength with 42 fs temporal duration and a spectral bandwidth of about 8.2 THz in a nitrogen atmosphere. The significant suppression of the laser intensity noise in mode-locked conditions by the random phase-matched SHG in the Cr:ZnSe crystal is experimentally demonstrated with respect to the multi-mode Er-fiber pump laser and the CW operational regime of the Cr:ZnSe laser. Despite the quite large intensity noise of the pump laser, the Kerr-lens mode-locked Cr:ZnSe is indeed characterized by a relative intensity noise of more than one order of magnitude lower. Even the phase noise of the pulse repetition frequency turns out to be limited by the relative intensity noise only for Fourier frequencies higher than 100 kHz. Finally, using an RF synthesizer, the repetition frequency of the Cr:ZnSe is also actively stabilized demonstrating a time jitter at a level of 1.6 ps for an integration bandwidth from 100 Hz to 100 MHz. The noise performance of the Cr:ZnSe KLM lasers shows, therefore, its reliability in high-sensitivity applications, such as broadband spectroscopy and precise chemical detection.

Funding

The authors acknowledge financial support by the European Union's NextGenerationEU Programme with the I-PHOQS Infrastructure [IR0000016, ID D2B8D520, CUP B53C22001750006] Integrated infrastructure initiative in PHOtonic and Quantum Sciences.

CRediT authorship contribution statement

Dario Giannotti: Writing – review & editing, Writing – original draft, Formal analysis, Data curation. **Antonio Caruso:** Writing – review & editing, Software, Formal analysis, Data curation, Conceptualization. **Fedele Pisani:** Writing – review & editing, Software. **Francesco Canella:** Writing – review & editing. **Niccolò S. Barberio:** Data curation. **Alessio Gambetta:** Writing – review & editing. **Nicola Coluccelli:** Writing – review & editing. **Yuchen Wang:** Writing – review & editing. **Paolo Laporta:** Writing – review & editing, Supervision. **Gianluca Galzerano:** Writing – review & editing, Writing – original draft, Supervision, Methodology, Conceptualization.

Declaration of competing interest

The authors declare that they have no known competing financial interests or personal relationships that could have appeared to influence the work reported in this paper.

Data availability

Data supporting the results presented in this paper are available from the authors upon reasonable request.

References

[1] F.K. Tittel, D. Richter, A. Fried, Mid-infrared laser applications in spectroscopy, in: Solid-State Mid-Infrared Laser Sources, Springer, 2003, pp. 458–529.
[2] J. Ma, Z. Qin, G. Xie, L. Qian, D. Tang, Review of mid-infrared mode-locked laser sources in the 2.0 μm–3.5 μm spectral region, Appl. Phys. Rev. 6 (2) (2019) 021317.
[3] Y. Zhang, K. Wu, Z. Guang, B. Guo, D. Qiao, Z. Wei, H. Yang, Q. Wang, K. Li, N. Copner, X. Li, Advances and challenges of ultrafast fiber lasers in 2–4 μm mid-Infrared Spectral Regions, Laser Photonics Rev. 18 (3) (2024) 2300786.
[4] I.T. Sorokina, E. Sorokin, Femtosecond Cr^{2+}-based lasers, IEEE J. Sel. Top. Quantum Electron. 21 (1) (2014) 273–291.
[5] S.B. Mirov, I.S. Moskalev, S. Vasilyev, V. Smolski, V.V. Fedorov, D. Martyshkin, J. Peppers, M. Mirov, A. Dergachev, V. Gapontsev, Frontiers of mid-IR lasers based on transition metal doped chalcogenides, IEEE J. Sel. Top. Quantum Electron. 24 (5) (2018) 1–29.
[6] I.T. Sorokina, E. Sorokin, T.J. Carrig, Femtosecond pulse generation from a SESAM mode-locked Cr:ZnSe laser, in: Conference on Lasers and Electro-Optics/Quantum Electronics and Laser Science Conference and Photonic Applications Systems Technologies, Optica Publishing Group, 2006, p. CMQ2.
[7] M. Baudrier-Raybaut, R. Haidar, P. Kupecek, P. Lemasson, E. Rosencher, Random quasi-phase-matching in bulk polycrystalline isotropic nonlinear materials, Nature 432 (2004) 374—-376.
[8] M. Yumoto, K. Miyata, Y. Kawata, S. Wada, Mid-infrared self-difference frequency generation via random quasi-phase-matching in Cr:ZnSe laser, Opt. Laser Technol. 169 (2024) 110161.
[9] A.E. Amili, M. Alouini, Noise reduction in solid-state lasers using a SHG-based buffer reservoir, Opt. Lett. 40 (7) (2015) 1149–1152.
[10] X. Bu, D. Okazaki, S. Ashihara, Inherent intensity noise suppression in a mode-locked polycrystalline Cr:ZnS oscillator, Opt. Express 30 (6) (2022) 8517–8525.
[11] M.N. Cizmeciyan, H. Cankaya, A. Kurt, A. Sennaroglu, Kerr-lens mode-locked femtosecond Cr^{2+}:ZnSe laser at 2420 nm, Opt. Lett. 34 (20) (2009) 3056–3058.
[12] M.N. Cizmeciyan, H. Cankaya, A. Kurt, A. Sennaroglu, Operation of femtosecond Kerr-lens mode-locked Cr:ZnSe lasers with different dispersion compensation methods, Appl. Phys. B 106 (2012) 887–892.
[13] Y. Wang, T.T. Fernandez, N. Coluccelli, A. Gambetta, P. Laporta, G. Galzerano, 47-fs Kerr-lens mode-locked Cr:ZnSe laser with high spectral purity, Opt. Express 25 (21) (2017) 25193–25200.
[14] N. Nagl, S. Gröbmeyer, V. Pervak, F. Krausz, O. Pronin, K.F. Mak, Directly diode-pumped, Kerr-lens mode-locked, few-cycle Cr:ZnSe oscillator, Opt. Express 27 (17) (2019) 24445–24454.
[15] Y. Wang, F. Fleming, R.A. McCracken, C. Liebig, S. McDaniel, G. Cook, P. Laporta, A.K. Kar, G. Galzerano, Hot-isostatic-pressed Cr:ZnSe ultrafast laser at 2.4 μm, Opt. Laser Technol. 154 (2022) 108300.
[16] H. Ostapenko, T. Mitchell, P. Castro-Marin, D.T. Reid, Three-element, self-starting Kerr-lens-modelocked 1-GHz Ti:sapphire oscillator pumped by a single laser diode, Opt. Express 30 (2022) 39624–39630.
[17] Z. Yu, H. Han, Y. Xie, Y. Peng, X. Xu, Z. Wei, CEO stabilized frequency comb from a 1-μm Kerr-lens mode-locked bulk Yb:CYA laser, Opt. Express 24 (2016) 3103–3111.
[18] W. Yao, Y. Wang, S. Ahmed, M. Hoffmann, M. van Delden, T. Musch, C.J. Saraceno, Low-noise, 2-W average power, 112-fs Kerr-lens mode-locked Ho:CALGO laser at 2.1 μm, Opt. Lett. 48 (2023) 2801–2801.
[19] R.P. Scott, T.D. Mulder, K.A. Baker, B.H. Kolner, Amplitude and phase noise sensitivity of modelocked Ti:sapphire lasers in terms of a complex noise transfer function, Opt. Express 15 (2007) 9090–9095.
[20] S. Vasilyev, K. Vodopyanov, M. Kolesik, S. Mirov, Using cross-phase modulation to transfer coherence between a Cr:Zns frequency comb and its optical pump, in: CLEO 2023, Technical Digest Series, 2023.
[21] T. Hirayama, M. Sheik-Bahae, Real-time chirp diagnostic for ultrashort laser pulses, Opt. Lett. 27 (10) (2002) 860–862.
[22] W. Yue, Y. Wang, C.-D. Xiong, Z.-Y. Wang, Q. Qiu, Intensity noise of erbium-doped fiber laser based on full quantum theory, J. Opt. Soc. Am. B 30 (2) (2013) 275–281.
[23] D.W. Allan, Statistics of atomic frequency standards, Proc. IEEE 54 (2) (1966) 221–230.